Brief Review

Modern Physics Letters B, Vol. 18, No. 15 (2004) 725–747
© World Scientific Publishing Company
World Scientific
www.worldscientific.com

FIRST-ORDER MAGNETIC PHASE TRANSITIONS AND COLOSSAL MAGNETORESISTANCE: JOINING MANGANESE PEROVSKITES AND MnAs

J. MIRA* and J. RIVAS

Departamento de Física Aplicada, Universidade de Santiago de Compostela, E-15782 Santiago de Compostela, Spain
**fajmirap@usc.es*

Received 10 June 2004

We revise some recent results on the nature of the magnetic phase transition of ferromagnetic manganese perovskites with colossal magnetoresistance. It is found that they exhibit first-order magnetic phase transitions mainly due to strong lattice effects. The presence of such first-order transition is strongly linked to the existence of a temperature region above the Curie Temperature with a phase-separated regime of coexisting metallic and insulating clusters. This situation is compared with that of MnAs, paradigm of system with first-order magnetic phase transition, and we observe a parallel phenomenology of these apparently different systems. This serves as a clue for the finding of a phase-separated regime also in MnAs and, moreover, for the finding of a colossal magnetoresistive effect similar to that of manganese perovskites.

Keywords: CMR; first-order magnetic phase transitions; magnetic phase transitions; manganites; MnAs.

1. Introduction

The investigation of the changes experienced by materials upon heating and, specifically, the situations that take place around their phase transitions (PT), are a major area of research in physics. Ferromagnetism has been often considered as a paradigm of second-order phase transition (SOPT), as in many cases the magnetization decreases in a continuous manner until it vanishes at the Curie temperature, T_C.

Nevertheless, there are few examples of ferromagnetic materials in which, at T_C, a true first-order phase transition (FOPT) is found instead.[1] In such a case, besides the abrupt variation of magnetization, other relevant alterations of the properties of the material take place.

In this review, we revise two relevant cases: manganese perovskites $La_{2/3}(Ca,Sr)_{1/3}MnO_3$ with colossal magnetoresistance (CMR) and MnAs. In principle, they seem very different, but the coincidence in the kind of transition makes them to behave similarly around T_C.

2. La(Ca,Sr)MnO

2.1. *Background*

Mn-based perovskites (A,B)MnO_3 (A = rare-earth, B = alkaline earth), present, at certain doping ranges, a ferromagnetic phase below T_C. The most studied cases are those of A = La with B = Ca and Sr. $La_{1-x}Ca_xMnO_3$ is ferromagnetic and insulator for low Ca doping and, for $0.20 < x < 0.50$, a ferromagnetic metal.[2] For B = Sr, the ferromagnetic phase is found for $x \geq 0.10$, which for $x < 0.17$ turns also into metallic.[3] In both, the maximum T_C takes place for $x = 1/3$, which means a rate $Mn^{3+}/Mn^{4+} = 2$. The maximum in T_C means that the ferromagnetic interaction is optimized at such doping value, which is not logical, because in principle it would be expected a maximum double exchange (DE) effect for $x = 0.5$. Besides, for $x = 2/3$, i.e. $Mn^{4+}/Mn^{3+} = 2$, the behavior should be the same as for $x = 1/3$, and it is not. All these facts reveal that there could be extra terms in the magnetic interaction.

In (La,Ca)MnO_3, several rich phenomena gather at the critical point: in addition to the ferromagnetic transition, the material changes from metallic to insulator,[2] anomalous thermal lattice expansions are measured[4] and, specially, huge changes of electrical resistivity under an external magnetic field (magnetoresistance) are detected.[5,6] The phenomenon, as commented in the introduction, was labeled by Jin *et al.*[6] as "colossal", and has been the decisive reason for the renaissance of the research activity on these materials since 1993.

It is thus evident that T_C is the first point to inspect if we are willing to discover the physics of the manganites. In the particular case of $La_{2/3}Ca_{1/3}MnO_3$, the large volume changes and the thermal hysteresis in resistivity around T_C led to think that a first-order transition was taking place. Lynn *et al.* found later, by neutron scattering investigations,[7] that the ferromagnetic transition was "unconventional". In a previous work, Hwang *et al.*[8] had proposed that in $La_{0.7}B_{0.3}MnO_3$ an abrupt change of the matrix element describing the electron hopping between Mn sites would cause an abrupt change in the double exchange coupling value and might be responsible for a first-order transition. Archibald, Zhou and Goodenough[9] generalized the conclusion to $A_{0.7}B_{0.3}MnO_3$ orthomanganites on the basis of a transition from polaronic to itinerant electrons, which would be reflected in a compensating discontinuous change in the mean potential energy, explaining a first-order decrease in the mean Mn–O bond length.

Nevertheless, despite the abovementioned contributions, some groups started to suggest[10] that the transition might be of second-order. Concretely, Lofland *et al.*,[11] by microwave absorption techniques, arrived to the conclusion that the ferromagnetic-to-paramagnetic transition of $La_{0.7}Sr_{0.3}MnO_3$ is continuous, of second-order. The apparent contradiction motivated an analysis[12] of the phase transition in mixed $La_{2/3}(Ca,Sr)_{1/3}MnO_3$ in order to detect if the different results are caused by interpretation errors or if there is any factor changing when passing from B = Sr to Ca.

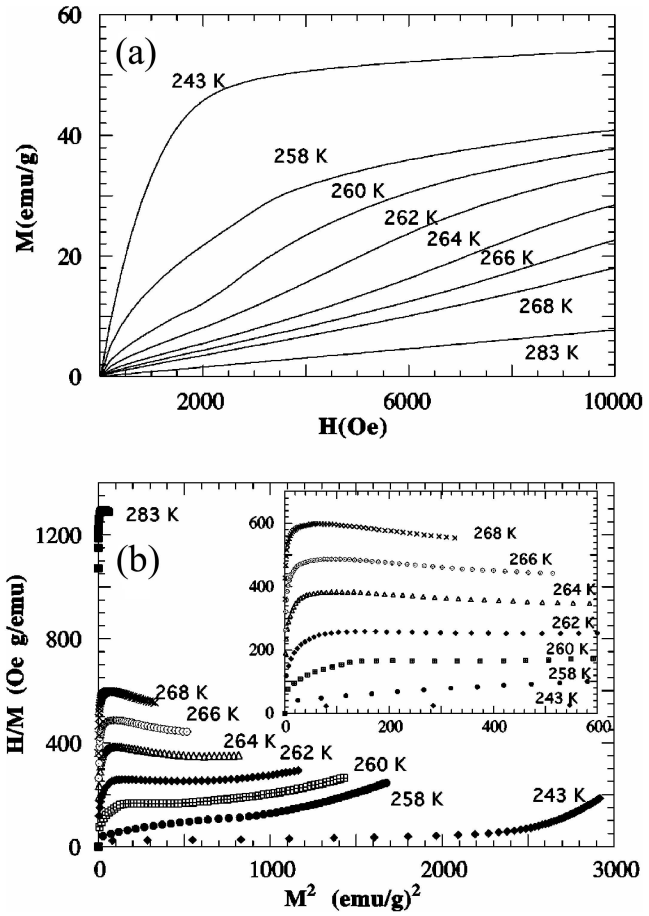

Fig. 1. (a) Magnetization versus magnetic field isotherms for $La_{2/3}Ca_{1/3}MnO_3$ in the vicinity of its T_C. Note the anomalies of slope at intermediate fields for isotherms between 258 and 268 K. (b) H/M versus M^2 plots of the above isotherms. It is clear the negative sign of the slope for some temperatures. The inset shows the detail for small values of M^2.

2.1.1. *Variation of the nature of the PT*

The problem to solve was to identify the type of PT: first- or second-order? To do this, we recovered[12,13] for the first time since the 60's (as far as we know), a criterion given by Banerjee,[14] that allows the determination of the order of a magnetic transition. Banerjee detected the essential similarity between the Landau–Lifshitz[15–18] and Bean–Rodbell[19] criteria and condensed them into one that provides a tool to distinguish first-order magnetic transitions from second-order ones by purely magnetic methods. It consists on the observation of the slope of isotherm plots of H/M versus M^2, being M the experimentally observed magnetization and H the magnetic field. A positive or negative slope indicates a second- or first-order transition respectively. We applied this to two compounds that have been at the center of

the controversy: $La_{2/3}Ca_{1/3}MnO_3$ and $La_{2/3}Sr_{1/3}MnO_3$.[12,20,21] Besides, intermediate compositions were analyzed, namely $La_{2/3}(Ca_{1-x}Sr_x)_{1/3}MnO_3$ materials with $x = 0$, 0.05, 0.15, 0.25 and 1, in order to observe the tendency between the two end members of the series. We note that in some of the literatures, a mention to $A_{0.7}B_{0.3}MnO_3$ instead of $A_{2/3}B_{1/3}MnO_3$ is made. In any case, in the framework of the phase diagram proposed by Urushibara *et al.*[3] for $La_{1-x}Sr_xMnO_3$, it is clear that variations from $x = 0.30$ to $x = 0.33$ are negligible, and the conclusions obtained for $x = 0.30$ are valid for $x = 0.33$. The same argument serves for the $x = 0.30$ and $x = 0.33$ Ca-doped samples.[2]

Low field magnetization versus temperature was first measured for both end members of the series, and gave estimations of their Curie temperatures, 260 K for $La_{2/3}Ca_{1/3}MnO_3$ and 370 K for $La_{2/3}Sr_{1/3}MnO_3$, both in agreement with data reported in previous literature.[7,11] In order to apply the Banerjee criterion, we measured initial magnetization isotherms in the vicinity of the critical points. Before each run, samples were heated above their T_C and cooled to the measuring temperature under zero field, in order to ensure a perfect demagnetization of the samples. Figure 1(a) shows the results for $La_{2/3}Ca_{1/3}MnO_3$. The first characteristic that calls our attention is the peculiar behavior of the curves at intermediate fields, where a decrease of slope followed by an increase is observed. This behavior near the critical point was observed by Bean and Rodbell in MnAs[19] (which presents a FOPT at T_C) and used by Banerjee to test his criterion. In Fig. 1(b), we applied it and obtained that H/M versus M^2 isotherms between 260 and 268 K present negative slopes in some parts, which according to the criterion is an indication of the first-order character of the transition.

When the same measurements in $La_{2/3}Sr_{1/3}MnO_3$ are done, it is seen that the isotherms (Fig. 2(a)) do not display the anomalous change of slope of the previous case. This difference is more clearly seen in the H/M versus M^2 plots of Fig. 2(b), where a positive slope for all the M^2 range is present.

Substitution of Ca by Sr causes an increase of T_C (Fig. 3(a)) as well as a decrease of the low field magnetization and a reduction of the differences between zero field cooled and field cooled M versus T curves. It is detected that the character of the transition is very sensitive to Sr-doping. Inspecting the Banerjee plot of Fig. 3(b), it can be seen that for $x = 0.05$, the material presents still a FOPT at T_C, but, attending to the slopes, such character is weaker than in $La_{2/3}Ca_{1/3}MnO_3$. In the case of $La_{2/3}(Ca_{0.85}Sr_{0.15})_{1/3}MnO_3$, the PT is already a second-order one (Fig. 3(c)).

When the properties of the end members of the series are compared, one of the main qualitative differences is that the transition at T_C is not accompanied by a metal-insulator transition in $La_{2/3}Sr_{1/3}MnO_3$.[3] Nevertheless, that does not seem to be a significative effect: $La_{0.8}Sr_{0.2}MnO_3$ does show a metal-insulator transition near T_C, and inspecting the Arrott plots[22] given by Lofland *et al.*[23] and Mohan *et al.*[24] it is clear that the magnetic transition is also of second-order for this composition.

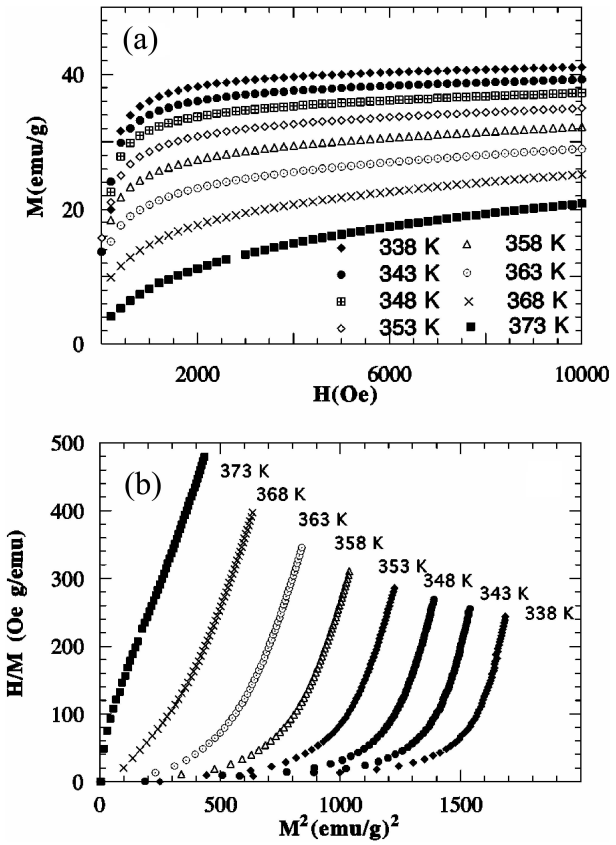

Fig. 2. (a) Magnetization versus magnetic field isotherms for $La_{2/3}Sr_{1/3}MnO_3$ in the vicinity of its T_C. (b) H/M versus M^2 plots for such isotherms. The slope is always positive, denoting the second-order character of the phase transition.

Therefore, it was concluded that although $La_{2/3}Ca_{1/3}MnO_3$ exhibits a first-order transition at T_C, $La_{2/3}Sr_{1/3}MnO_3$ does not. Therefore, the existence of a first-order transition for the $A_{2/3}B_{1/3}MnO_3$ orthomanganites, irrespective of the identity of A or B cannot be stated. We recovered also a powerful tool for the recognition of magnetic FOMT, further applied successfully to other systems.[25]

All these scenarios created debate and controversy, because depending on the compound studied, different interpretations were made. Then, the main issue to address is: what makes such similar compounds to behave so differently? In the search for an answer, the series was analyzed by means of calorimetric, dilatometric and resistivity measurements.[26,27] Differential Scanning Calorimetry (DSC), a technique that allows the identification of first- and second-order phase transitions of the samples, shows a very interesting evolution with Sr-doping (Fig. 4).

For $La_{2/3}Ca_{1/3}MnO_3$, the curve shows the presence of two phase transitions: a first-order one, at the Curie temperature, and another at about 345 K, whose

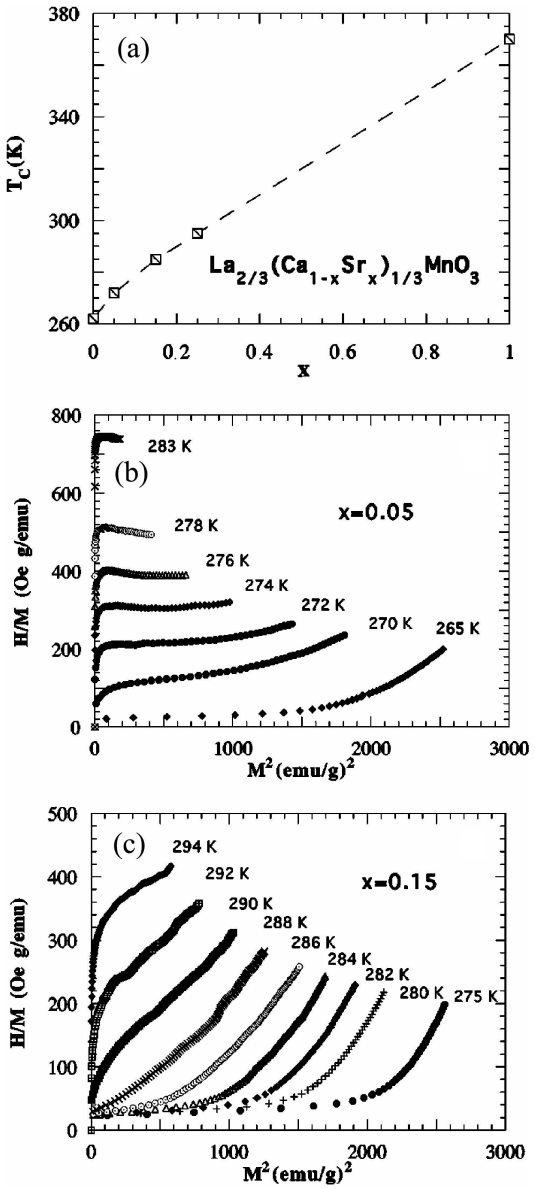

Fig. 3. (a) Dependence of the Curie temperature, T_C, on the Sr-doping degree, x. (b) H/M versus M^2 plots of isotherms in the vicinity of the Curie point of $La_{2/3}(Ca_{0.95}Sr_{0.05})_{1/3}MnO_3$. (c) H/M versus M^2 plots of isotherms in the vicinity of the Curie point of $La_{2/3}(Ca_{0.85}Sr_{0.15})_{1/3}MnO_3$.

nature is yet to be elucidated (although in principle, it seems to be a second-order one). $La_{2/3}(Ca_{0.95}Sr_{0.05})_{1/3}MnO_3$ presents a similar behavior. But, for higher x, only one phase transition of second-order is detected. This second-order transition is present in all the samples. The change from first- to second-order character is in

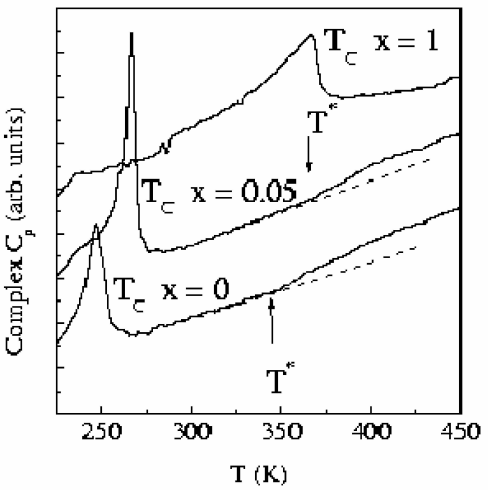

Fig. 4. Complex heat capacity curves of $La_{2/3}(Ca_{1-x}Sr_x)MnO_3$ with $x = 0$, 0.05 and 1. For $x = 0$ and 0.05, a first-order transition at T_C is followed by a slight second-order one at T^*, marked with arrows. For $x = 0.15$, only a clear second-order one is present, at T_C.

agreement with the results of Ref. 12. We think that the origin of this difference must be searched in an aspect not considered (to our knowledge) till now. Two perovskite structures (with space groups *Pbnm* and $R\bar{3}c$) exist in the samples analyzed here. The $x = 0$ and 0.05 samples belong to the *Pbnm* space group, with practical invariance of the structural parameters. However, for $x \geq 0.15$ we observe a transition to the $R\bar{3}c$ space group. That is, the change of space group happens at a tolerance factor value, $t \simeq 0.92$ (t defined in a perovskite $AMnO_3$ as: (A–O)/$\sqrt{2}$ (Mn–O)). And the key point is that, whereas long range Jahn–Teller (JT) distortions are possible in the *Pbnm* phase,[28,29] the higher symmetry of the MnO_6 octahedra in the $R\bar{3}c$ phase (with a unique Mn-O bond length) does not allow them (the JT distortion modes are tetragonal or orthorhombic: rhombohedral symmetry does not split the *e*-orbital degeneracy). Accordingly, only local JT distortions have been observed in $La_{1-x}Sr_xMnO_3$ with $x < 0.35$.[30] JT distortions may assist polaron formation,[7,30] which causes the anomalous volume change detected by magnetostriction measurements in $La_{2/3}Ca_{1/3}MnO_3$.[4] (Volume change is also one of the ingredients of a first-order transition.[19]) In this context, dilatometry experiments carried out in $La_{2/3}(Ca_{1-x}Sr_x)_{1/3}MnO_3$[26,27] showed different behaviors around T_C above and below the critical tolerance factor $t = 0.92$ (Fig. 5(a)): the anomalous volume expansion of $La_{2/3}Ca_{1/3}MnO_3$ does not take place in $La_{2/3}Sr_{1/3}MnO_3$.

Also, volume sensitivity to a magnetic field (magnetovolume effect), a signature of the existence of magnetic polarons, is high for $La_{2/3}Ca_{1/3}MnO_3$ ($t < 0.92$) and negligible for $La_{2/3}Sr_{1/3}MnO_3$ ($t > 0.92$), as seen in Fig. 5(b). This means that, whereas $La_{2/3}Ca_{1/3}MnO_3$ shows (magnetic) polaronic effect, $La_{2/3}Sr_{1/3}MnO_3$

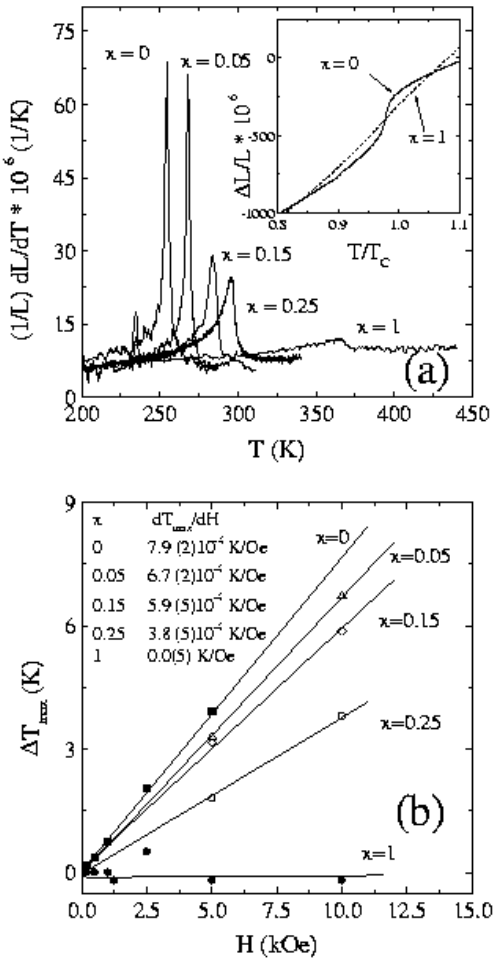

Fig. 5. (a) Inset: dilation versus normalized temperature of $La_{2/3}Ca_{1/3}MnO_3$ and $La_{2/3}Sr_{1/3}MnO_3$. Note the anomalous thermal expansion at T_C in the $x = 0$ case, and the practical absence of such anomaly in the $x = 1$ one. Main frame: derivative of the dilation curves of the $La_{2/3}(Ca_{1-x}Sr_x)_{1/3}MnO_3$ series. The anomalous thermal expansion is much sharper and symmetric for the $x = 0$ and 0.05 samples ($t < 0.92$) than in the other cases. Also note the absence in the Ca-rich compounds of the long "tail" apppearing below T_C in $x = 0.15$ samples, which is characteristic of second-order transitions in 3D systems (see also Fig. 1). (b) Shift of the peak of the derivative of the dilation measurements under magnetic field. The shift is monotonically reduced with x until $x = 1$, for which it is negligible.

does not. For manganites with $t < 0.92$, the static, cooperative JT deformations are replaced in the ferromagnetic phase by dynamic ones, which introduce vibrational modes into the spin-spin interaction.[31] A dynamic JT deformation gives isotropic ferromagnetic order between Mn^{3+} ions by superexchange. Therefore, in $La_{2/3}Ca_{1/3}MnO_3$, a material considered historically as example of ferromagnetic coupling due to the double exchange mechanism (DE),[32–34] two interactions,

superexchange and double exchange, do indeed play a role.[35] At T_C, the JT distortion becomes static and cooperative, causing the extra superexchange term to disappear abruptly. At the same time, the *e*-electrons localize, but the ferromagnetic interactions between Mn sites keep on active in short range zones via Zener DE (to be distinguished from the de Gennes DE), with a coupling constant $J > k_B T_C$. The consequence is that a superparamagnetic second phase segregates above T_C. This phase is present until a temperature $T^* > T_C$, which would be the Curie temperature of the system if it were a pure double exchange ferromagnet (i.e. if the first-order transition were not present at lower temperatures). For $La_{2/3}Ca_{1/3}MnO_3$, the transition within the ferromagnetic clusters is detected by us at $T^* \simeq 345$ K (of the order of the Curie temperature of $La_{2/3}Sr_{1/3}MnO_3$, 360 K) in the DSC curve of Fig. 4. The magnetic polarons above T_C would then be a consequence of the clustering with an anomalously high coupling constant, J, not understandable in the context of a conventional cluster model. Instead, for $La_{2/3}Sr_{1/3}MnO_3$ the paramagnetic part can be fitted with a cluster model, because its T_C is the one imposed by the overcoming of the DE interaction by pure thermal energy, and the ferromagnetic interactions above T_C are the usual for a ferromagnet. For this reason, Viret *et al.*[36] do not find anything of special relevance in materials like $La_{0.75}Sr_{0.25}MnO_3$ with $t > 0.92$. The change from *Pbnm* to $R\bar{3}c$ brings about considerable variations in many physical properties. For example, the magnetic entropy change (magnetocaloric effect), $\triangle S_M$, was measured at T_C in all the samples,[37] and it is presented in Fig. 6(a). It is observed that $x = 0$ and $x = 0.05$ compounds (*Pbnm*) show large magnetic entropy changes, similar to the results reported by Guo *et al.*,[38] but, for $x \geq 0.15$ it is considerably smaller. Guo *et al.* attribute the large $\triangle S_M$ in Ca-doped $LaMnO_3$ to the sharp volume change at T_C. Taking into account that the $x = 0$ and $x = 0.05$ samples both exhibit a large volume expansion and the $x \geq 0.15$ does not, our results seem to confirm their hypothesis.

The magnetoresistive properties are also dramatically affected when changing from *Pbnm* to $R\bar{3}c$. Figure 6(b) shows how it is more pronounced in $x = 0$ and $x = 0.05$ than in the others. It is worth mentioning how closely this variation correlates with $\triangle S_M$ and the maximum dilation values (Fig. 6(c)). Some other noticeable variations, related to crystal symmetry, like a crossover from anisotropic to isotropic electronic transport, have also been reported recently.[39] With this idea in mind, we propose that the phase diagram of Hwang *et al.*[8] for $Re_{0.7}A_{0.3}MnO_3$ should be reformed, taking into account a new phase boundary at $t = 0.92$. This is a crucial boundary for a correct and whole description of manganese perovskites, because it separates "pure" DE systems ($t > 0.92$) from those that are not ($t < 0.92$), due to lattice effects. For $t < 0.92$, the JT distortion is causing the disappearance of the global magnetic order below the temperature expected according to the intensity of the exchange coupling constant. Zhang and Bishop[40] have already proposed that lattice effects decrease the T_C of the "pure" DE system. Both Zhao *et al.*[41] and Hwang *et al.*[8] had detected the importance of the ionic radii on the

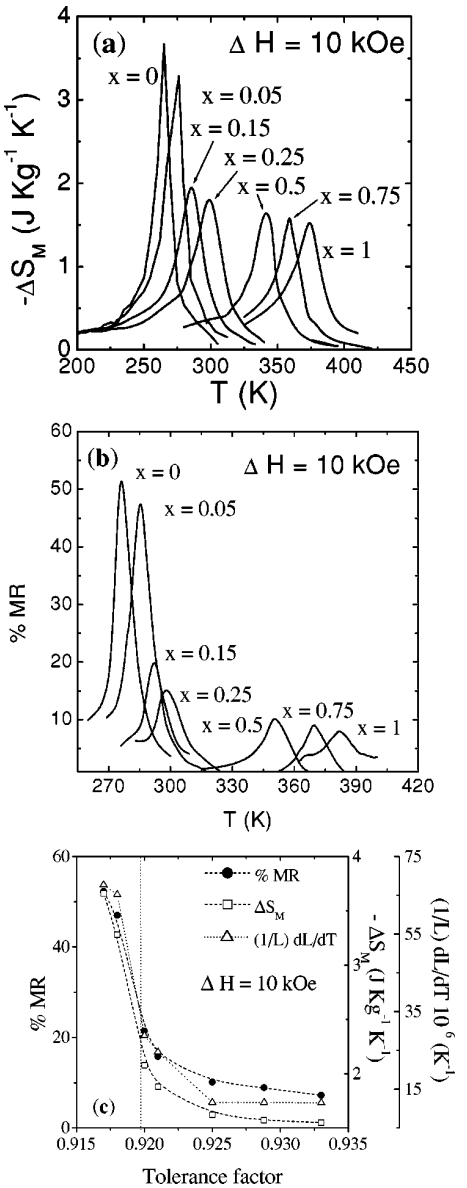

Fig. 6. (a) $\triangle S_M$ versus temperature of the $La_{2/3}(Ca_{1-x}Sr_x)MnO_3$ series, for a magnetic field change from 0 to 10 kOe. (b) Magnetoresistance versus temperature for the same samples as in (a). (c) Comparison of the evolutions of both $\triangle S_M$, MR and maximum dilation of the whole series versus tolerance factor.

properties of these perovskites, but they did not take into account the important role of the crystal structure and they did not relate it with the observed physical properties. Concretely, Zhao *et al.*[41] observed a rapid increase of the isotope exponent with decreasing the average ionic radius at the $Re_{1-x}A_x$ site.

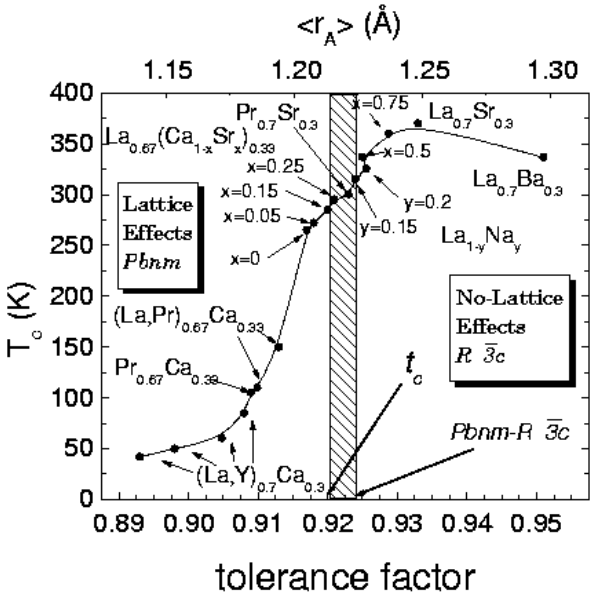

Fig. 7. T_C versus tolerance factor phase diagram for $Re_{1-x}A_xMnO_3$. Results for $La_{1-x}Na_xMnO_3$ samples are taken from Ref. 43. The shadowed area separates compounds showing not only different structural phases but also different types of magnetic phase transitions. This frontier also delimitates the importance of lattice effects, much more relevant for compounds on the left hand side of this phase diagram. Magnetic polarons/phase separation, isotopic effect, first-order transitions at T_C, very high MR, large magnetic entropy changes, and anomalous and magnetic field dependent thermal expansion around T_C, are also limited to the left part of this diagram.

In the framework of our reasoning, this is the consequence of activating lattice effects. In the diagram of Fig. 7 we summarize this idea representing together our data and other available from the literature. It is worth mentioning those by Radaelli *et al.*,[42] where a similar t for the structural phase change is stated, and those by Savosta *et al.*,[43] who measured continuous second-order phase transitions in Na doped $LaMnO_3$. These latter results are in agreement with our phase diagram, as they all have $t > 0.92$.

2.2. *The $T_C < T < T^*$ region*

The region between T_C and T^* is somewhat intringuing and is probably the basis of many of the anomalous effects found in these kinds of systems. In order to explain such behavior, the idea of phase separation, i.e. the coexistence of regions of localized and itinerant carriers within the same crystallographic structure, has been proposed.[44,45] In this framework, Dagotto, Hotta and Moreo[46] proposed in a recent review the existence of a temperature window where coexisting metallic and insulating clusters appear above the Curie temperature, T_C, when this transition is first-order and there is a source of disorder. This temperature window would extend

up to $T^* > T_C$, where these clusters dissociate to form two-Mn Zener polarons (or small polarons).

This idea is completely coincident with ours, therefore, with the aim of defining better the existence of the $T_C < T < T^*$ region, ultrasonic attenuation and phase velocity measurements were carried out in $La_{2/3}Ca_{1/3}MnO_3$ and $La_{2/3}Sr_{1/3}MnO_3$.[47] This technique is proved to be a very sensitive tool not only for studying defects and microscopic processes in solids, but also for probing systems undergoing magnetic and structural phase transitions.

In Fig. 8(a), we show ultrasonic velocity versus temperature data for $La_{2/3}Ca_{1/3}MnO_3$ and $La_{2/3}Sr_{1/3}MnO_3$, and attenuation versus temperature data for $La_{2/3}Ca_{1/3}MnO_3$, obtained with 5 MHz transversal waves between 220 and 400 K. For $La_{2/3}Sr_{1/3}MnO_3$ it was impossible to measure the attenuation because of its high value allowed to obtain only two echoes at room temperature

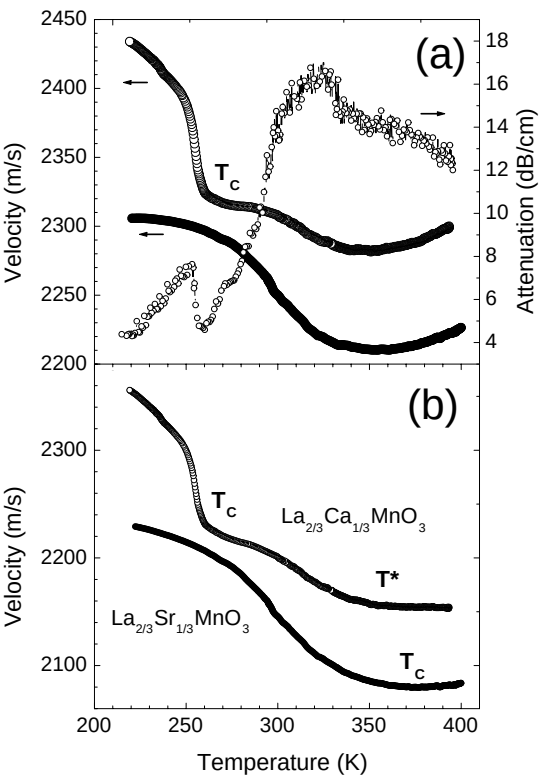

Fig. 8. (a) Transversal ultrasonic velocity versus temperature of $La_{2/3}Ca_{1/3}MnO_3$ (open symbols) and $La_{2/3}Sr_{1/3}MnO_3$ (filled symbols), and attenuation versus temperature of $La_{2/3}Ca_{1/3}MnO_3$ (attenuation not measurable in LaSrMnO), as measured. (b) Ultrasonic velocity versus temperature for the same samples after background substraction. Note the steep decrease of velocity as well as the peak in attenuation at the T_C of LaCaMnO. Note also the similar velocity anomalies in the region 350–370 K, corresponding to T^* in LaCaMnO and to T_C in LaSrMnO.

(at higher temperatures the second echo became negligible). The transit time was measurable at room temperature, and then time variations were measured. The influence of thermal expansion was not taken into account, because it is negligible: if $(\delta l)/l = 2 \cdot 10^{-4}$ we have that for our sample, with $l = 2.4$ mm thick (4.8 mm microwave path) and a velocity of about 2500 m/s, δt (t = time) is $5 \cdot 10^{-4}$ s and therefore, at T_C, the associated variation of velocity is far smaller than the one we measured.

In our original ultrasonic velocity data, an approximately linear increment with temperature was observed at temperatures above 350 K for both samples. At this temperature range, no mechanism related with magnetic phase transitions is expected, and this variation should be attributed to another mechanism, as the produced by crystalline defects present in the material. This component must be substracted from original data, in order to obtain the true transition temperatures. As is well-known,[48] dislocation lines present in the material can oscillate driven by an oscillatory applied stress, showing a resonant behavior. From experimental data and the kink picture for dislocation anelasticity, Moreno–Gobbi and Eiras[49] have shown, working on crystalline copper, that this resonant mechanism gives a term proportional to T for velocity and proportional to T^2 for attenuation in the temperature interval investigated in the present work. The coefficient of proportionality depends on L^2 for velocity and L^4 for attenuation, where L is the average free length of the segment of dislocation lines. We assumed a background of this kind in order to take into account the behavior of velocity observed at high temperatures. The velocity background was fitted to the high temperature region of velocity versus temperature curves, and then substracted from original data. These fits gave a term 0.37 T for LaCaMnO and 0.46 T for LaSrMnO. The so-corrected velocity data are presented in Fig. 8(b). The differences between the numerical values of the coefficients of proportionality have their origins in the different values of L expected for different materials.[48]

The ultrasonic velocity for $La_{2/3}Ca_{1/3}MnO_3$ presents two clear anomalies: an abrupt hardening at about 250–260 K, and another lesser at about 350–360 K. The first one marks the T_C of this system[7,8,12,26,50] ($T_C = 260$ K). The behavior is similar to that found at MHz frequencies by other authors,[51,52] and at kHz frequencies by Cordero *et al.*[53] The abrupt decay of the curve at T_C signals the first-order character of this transition,[54] an interpretation that is in agreement with results obtained from other techniques.[7,8,12,26,50] The decay in velocity is accompanied by a peak in the attenuation curve at T_C. This peak is asymmetric, in agreement with the results of Cordero *et al.*,[53] who explain it invoking the presence of inhomogeneous phases below T_C in a similar way to relaxor ferroelectrics.[55,56]

The second anomaly takes place above T_C, showing a hardening process at $T^* \simeq 350$–360 K (Fig. 9). In Fig. 8, it is also observed a very large attenuation peak at 320 K accompanying this velocity anomaly. This was not observed by Cordero *et al.* at kHz frequencies, but is clearly observed in our MHz measurements. The

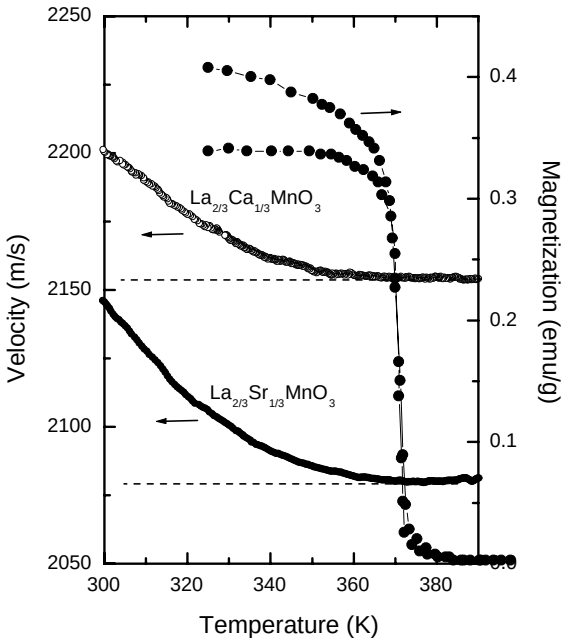

Fig. 9. Detail of the corrected transversal ultrasonic velocity versus temperature of $La_{2/3}Ca_{1/3}MnO_3$ and $La_{2/3}Sr_{1/3}MnO_3$ in the T^* region. For comparison, magnetization versus temperature data (zero-field-cooled and field-cooled) of $La_{2/3}Sr_{1/3}MnO_3$ are included.

reason lies on the higher sensitivity of MHz techniques to small inhomogeneities, as magnetic clusters, due to the shortest wavelength (approximately 0.5 mm at 5 MHz for transversal waves).

In Figs. 8 and 9, it is also observed that the only noticeable anomaly in the utrasonic velocity curve of $La_{2/3}Sr_{1/3}MnO_3$ is a hardening process beginning at about 370 K (in the order of that of LaCaMnO in the same temperature region), that is coincident with the second-order phase transition point of this compound, clearly observed by magnetization measurements ($T_C \simeq 370$ K).[10,12] In the explored temperatures, no more transitions were detected. Based on this behavior, we can perfectly associate the process of hardening observed at 370 K to this second-order phase transition.

From our ultrasonic velocity data, it seems that this phase is different in the two systems considered, as expected from our previous results, and confirmed the existence of a transition point at $T^* > T_C$ in LaCaMnO. It is worth mentioning that our T^* is similar to the point at which both the volume thermal expansion deviates from a Gruneisen fit and the inverse magnetic susceptibility deviates from a Curie–Weiss fit, after results of de Teresa *et al.* in $La_{2/3}Ca_{1/3}MnO_3$ (Ref. 57). Supporting our results, we have to mention that neutron diffraction studies[36] in the paramagnetic region of $La_{2/3}Sr_{1/3}MnO_3$ show differences with respect to $La_{2/3}Ca_{1/3}MnO_3$. We also want to call the attention on the similar values of the temperatures of the

second-order transitions, $T^* \simeq 350$–360 K for $La_{2/3}Ca_{1/3}MnO_3$, and $T_C \simeq 370$ K for $La_{2/3}Sr_{1/3}MnO_3$. Again, this leads to think that the magnetic interaction between the Mn atoms is of the same strength in both compounds and only the occurrence of the first-order change in LaCaMnO is breaking the long-range order at a temperature below T^*.

The anomaly at T^* shows that the magnetic phase transition is not from ferromagnetism to a purely paramagnetic state, but some sort of magnetic structure is present. Such idea is in accordance with the theoretical results of Moreo *et al.*,[58] who have proposed, after computer simulations, that large coexisting metallic and insulating clusters of equal electronic density are generated in manganese oxides with first-order magnetic transitions. Kimura *et al.*[59] have qualified these compounds as relaxor ferromagnets, with a relaxation from one phase to the other. The fluctuations between both phases have been seen by Transmission Electron Microscopy by Podzorov *et al.*[60] In such a case, after Kimura *et al.*[59] the transition would be diffuse, like the one observed by us at T^*. Nowadays, there is many experimental work that leads to assume the electronic phase-separated nature of such materials, and now it is well established that this phase separation is not due to chemical inhomogeneities or to the existence of phases with a different chemical composition.[61] Rivadulla *et al.* have suggested that vibrational anisotropy (between Q_2 and Q_3 Jahn–Teller modes) can be at the origin of the phase separation mechanism, after analyzing the role played by vibrational anisotropy on orbital and charge ordering.[62] Although this approach is quite recent in manganese perovskites, it had already been proposed by Señarís Rodríguez and Goodenough[63] and some of us[64,65] to explain the magnetic and electrical properties of Sr-doped cobalt perovskites, thinking of a percolative transition at T_C.[66–68]

3. MnAs

3.1. *Background*

MnAs is a material whose ferromagnetic character has been known since long time ago.[69,70] It was the first case studied of ferromagnetic transition of first-order[19] and, in fact, it is the textbook paradigm of such phenomenon in magnetism. At its $T_C = 313$ K, where the latent heat associated to the transition is 1.79 cal/K,[71] several changes are observed in the physical properties, similar to that found in CMR manganites: metal-insulator transition,[72,73] a large volume change of 1.86%,[74] consequently, a high magnetocaloric effect. Above T_C, a second-order phase transition is observed at $T^* = 399$ K.[75]

Between T_C and T^*, the magnetic susceptibility increases with temperature,[72,76] transforming to a Curie–Weiss law above T_t. X-ray diffraction studies[77] revealed a change in the crystallographic arrangement at the first-order transition point, from the NiAs-type ($B8_1$) hexagonal structure to the MnP-type ($B31$) orthorhombic one. The orthorhombic distortion decreases with increasing temperature and the hexagonal $B31$ structure reappears above T_t. It was soon recognized that a cross-

over from high to low spin states on the manganese site could occur on going from the $B8_1$ to the $B31$ structure.[78] Studies of the influence of higher hydrostatic pressure on MnAs led to a modification of the Bean–Rodbell theory.[75,79] The spin-state instability appears to be responsible for a giant magnetoelastic response reported recently by Chernenko *et al.*[80]

3.2. *Phase separation and CMR*

The phenomenology described above and that described for the CMR manganites are quite parallel, and led us to suspect of a behavior of MnAs even much more alike to manganites, which might include a phase separated state between $T_C < T < T^*$ and CMR in that region. Then, we first performed a study of the stability of the orthorhombic $B31$ phase in an applied magnetic field.[81] At room temperature, below $T_C = 313$ K, the diffraction pattern was that of the hexagonal $B8_1$ phase (space group $P6_3/mmc$) with lattice parameters ($a = 3.7187(5)$ Å, $c = 5.7024(5)$ Å at $T = 300$ K) in agreement with those reported by Willis and Rooksby.[74] Reflections belonging to the orthorhombic $B31$ structure described by Wilson and Kasper[77] appeared above T_C. Figure 10 shows the evolution of the diffraction pattern as the temperature is increased from 312 K to 317 K. The hexagonal and the orthorhombic phases coexist between 313 and 315 K, whilst the whole sample is in the orthorhombic phase at 317 K.

The sample was then heated at 321 K, and equilibrated at that temperature for two hours in zero field. The magnetic field was then increased at regular steps up to

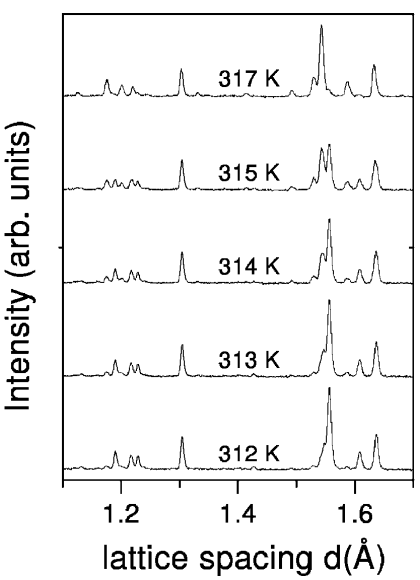

Fig. 10. Temperature dependence of the MnAs diffractogram in a selected d spacing range. The hexagonal-orthorhombic transition starts at 313 K and is completed at 317 K.

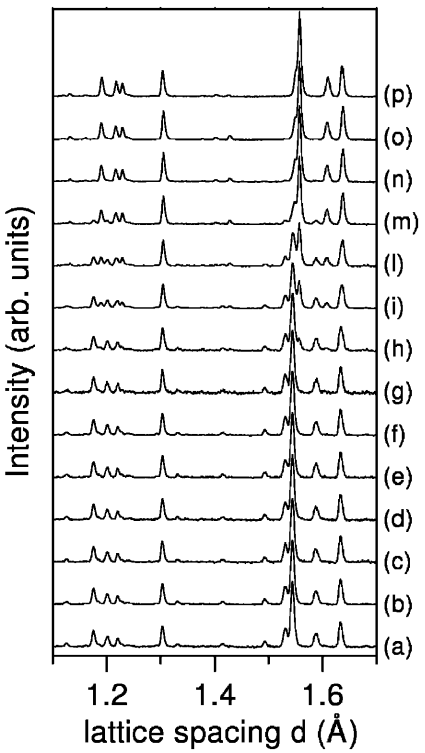

Fig. 11. Magnetic field dependence of a selected region of the diffraction pattern recorded at 321 K, showing the evolution from the orthogonal to the hexagonal form of MnAs; (a) B = 0 T; (b) B = 0.50 T; (c) B = 1.00 T; (d) B = 1.50 T; (e) B = 2.00 T; (f) B = 2.75 T; (g) B = 3.00 T; (h) B = 3.50 T; (i) B = 3.75 T; (l) B = 4.00 T; (m) B = 4.50 T; (n) B = 5.00 T; (o) B = 5.50 T; (p) $T = 300$ K, B = 0 T.

5.5 tesla and the diffractograms recorded at each step. The results are reported in Fig. 11. It is readily apparent that the diffraction profile is substantially modified as B increases above 3.5 T, and that the hexagonal phase is fully restored at B = 5 T. Indeed, diffractograms *o* (321 K, B = 5.5 T) and *p* (300 K, B = 0) in Fig. 11 are practically undistinguishable. The extent of the orthorhombic distortion decreases continuously as B increases, nearly vanishing by B = 5.0 T.

The magnetic field evolution of the diffraction pattern has also been measured at 319 and 318 K. With decreasing temperature, the phase transformation occurs at smaller values of the magnetic field (2.5–4.0 T at 318 K, 3.0–4.5 T at 319 K). The neutron diffraction data do not show a sharp transition, but rather the coexistence of two phases with the growth of the ferromagnetic phase at the expense of the paramagnetic $B31$ phase as B increases. Growth of the ferromagnetic phase is possible because the $B31$ phase is derived from the $B8_1$ phase by a cooperative displacement of pairs of [1, −1, 0] rows toward one another to form stronger Mn–Mn bonds, across shared octahedral-site edges in zig-zag chains within the basal planes.

These displacements also create shorter Mn–As bonds, which raises the antibonding states that σ-bond to the As atoms and triggers the transition to a low-spin state.[79]

Extrapolation of the Brillouin temperature dependence of the magnetization of the $B8_1$ phase to the above first-order transition at T_C gives a fictitious Curie temperature $T_C^* = 388$ K. Since an applied magnetic field B stabilizes the high-spin, ferromagnetic phase relative to the $B31$ paramagnetic phase, a global insulator-metal $B31$–$B8_1$ transition might be induced by B in the interval $T_C < T < T_C^*$. Alternatively, if $B8_1$ regions exist within a $B31$ matrix in the interval $T_C < T < T_t$, we can expect that below T_C^* the ferromagnetic $B8_1$ regions will grow in a magnetic field at the expense of the paramagnetic $B31$ matrix to beyond the percolation threshold. In either case, a CMR would occur between T_C and T_C^*. If the B field induces a global $B31$–$B8_1$ transition, it would give a CMR analogous to that found, for example, at the metamagnetic transition of the charge and orbital-ordered CE phase of the perovskite $Nd_{0.5}Sr_{0.5}MnO_3$.[82] If, on the other hand, the magnetic field nucleates and/or grows the $B8_1$ phase, it would give a CMR phenomenon analogous, for example, to that of the perovskite system $(La_{0.7-x}Pr_xCa_{0.3})MnO_3$.[8] However, whereas the CMR occurs in the manganese oxides at a too low temperature to be technically practical, it would occur in MnAs at a little above room temperature and could be easily adjusted to operate at room temperature by small compositional changes.

Figure 12 shows the enhanced magnetoresistance response of MnAs measured in the predicted temperature range, $T_C < T < T_C^*$. Almost the same results were obtained for both samples used in this study. Although the absolute value of the

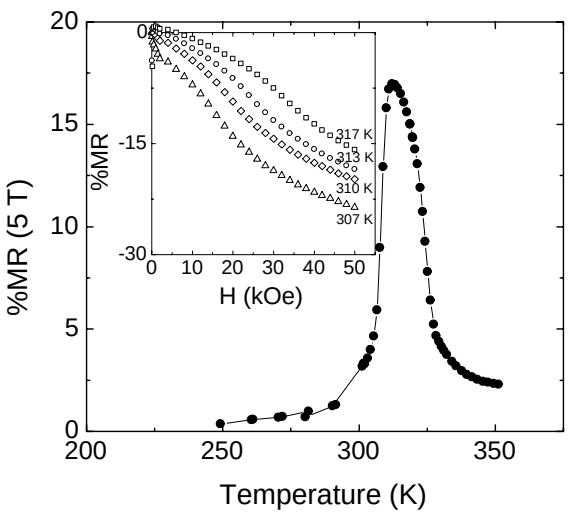

Fig. 12. Magnetoresistance (MR = $[\rho(0) - \rho(5\text{T})/\rho(0)] \times 100$) versus temperature of MnAs. Inset: MR versus B.

magnetoresistance is not as large as in other compounds like $La_{2/3}Ca_{1/3}MnO_3$,[6] we call it a CMR-like to highlight the common origin with that in the manganites.

It is clear that the origin of this MR effect is intrinsic and not due to an intergranular process in a material with a high spin polarization. This is reflected (besides of the independence of the result on sample synthesis) in an almost straight field dependence of the MR (see the inset of Fig. 12) and the almost temperature independent MR below the peak centered at T_C. Analogies between the behavior of MnAs in a magnetic field above T_C and that of the manganese-oxide perovskites are noteworthy. In the manganese perovskites, the σ-bonding d electron of a high-spin octahedral site Mn(III) ion occupies a twofold-degenerate pair of e-orbitals. This e-orbital degeneracy is removed by a local distortion of the $MnO_{6/2}$ octahedron; and at lower temperatures and high Mn(III) concentrations, the local distortions are ordered cooperatively so as to minimize the associated elastic energy. A recent study of $LaMn_{1-x}Ga_xO_3$[83] has shown that in this single-valent system, dilution of the Mn(III) atoms suppresses the orbital ordering in local ferromagnetic regions; a vibronic superexchange is ferromagnetic whereas the orbitally ordered matrix is antiferromagnetic. In this system, application of B disorders the orbital order of the matrix to transform a spin glass to a ferromagnet.[83] In the mixed-valent perovskite system $La_{1-x}Sr_xMnO_3$, an orthorhombic-rhombohedral structural phase transition is induced by an external magnetic field for $x = 0.17$.[84] This transition involves a change from [1, −1, 0] to [1, 1, 1] of the axis of cooperative rotation of the $MnO_{6/2}$ octahedra. A crossover from localized to itinerant behavior of the σ-bonding e-electrons occurs in the compositional interval $0.1 \leq x \leq 0.17$.[85] In this interval, hole-rich ferromagnetic regions are segregated from a hole-poor paramagnetic matrix in the paramagnetic temperature range $T_C < T \leq 300$ K by cooperative oxygen displacements. The hole-rich regions are mobile, and they grow in a B to beyond a percolation threshold by B = 5 T to give the CMR-like phenomenon. In the interval $0.1 \leq x \leq 0.15$, the transition at T_C is first-order; and in a narrow temperature range $T_{OO} < T < T_C$, the orbitals undergo a rearrangement to another type of order below T_{OO}. Near $x = 0.1$, the interval $T_{OO} < T < T_C$ narrows, and the matrix remains orbitally ordered in zero magnetic field to give spin-glass behavior typical of ferromagnetic clusters having a T_C greater than the Néel temperature of the matrix. However, the orbitals of the matrix become disordered in a modest B to give ferromagnetic order below a T_C.

All match quite well with the scenario that we have been proposing up to now. Goodenough[35] has invoked the virial theorem to make the same deduction for the manganese-oxide perovskites at the crossover from localized to itinerant behavior of the σ-bonding electrons. However, MnAs is single-valent, so the analogy with $LaMn_{1-x}Ga_xO_3$ is more appropriate even though this perovskite remains insulating in the ferromagnetic phase. In MnAs, the basal-plane orbitals on the Mn atoms are half-filled, and the electrons approach the crossover from localized to itinerant electronic behavior. In the paramagnetic $B31$ phase, the Mn atoms become displaced

below T_t so as to form stronger Mn–Mn bonds in the zig-zag chains and weaker Mn–Mn bonds between the chains. These displacements not only order the Mn–As bonding so as to induce the low-spin state, but they also represent an ordering of the in-plane Mn–Mn bonds that changes the translational symmetry so as to split the basal-plane band at the Fermi energy. Ferromagnetic interactions by the other d electrons are dominant, but these interactions are weakened by the transition to the low-spin state, which reduces the Mn–Mn separation and strengthens the in-plane Mn–Mn bonding. Since no bonding occurs between half-filled orbitals with parallel spins, stabilization of the high-spin ferromagnetic $B8_1$ phase suppresses in-plane Mn–Mn bonding and increases the in-plane Mn–Mn separation. Stabilization of the ferromagnetic phase in a B with removal of the in-plane Mn–Mn bonding is to be compared with suppression by a B of the orbital ordering at the Mn(III) ions in $LaMn_{1-x}Ga_xO_3$. This is the first crystallographic transition induced by a magnetic field that involves breaking of metal-metal bonds rather than orbital disorder.

4. Conclusions

The new ideas and conjectures formulated during the last decade in connection with the study of the colossal magnetoresistance (CMR) response in Mn perovskites might be expanded to other systems. Among these ideas is the invocation of a phase separation scenario that might be of particular relevance in other systems, like MnAs, where first-order phase transitions occur.

Acknowledgments

The DGI of the Ministry of Science of Technology of Spain is acknowledged for financial support under project FEDER MAT2001-3749. We also wish to acknowledge all our laboratory colleagues and co-workers for their contributions to the research lines described in this review.

References

1. S. V. Vonsovskii, in *Magnetism*, Vol. 2 (Wiley, New York, 1974).
2. P. Schiffer, A. P. Ramírez, W. Bao and S.-W. Cheong, *Phys. Rev. Lett.* **75** (1995) 3336.
3. A. Urushibara, Y. Moritomo, T. Arima, A. Asamitsu, G. Kido and Y. Tokura, *Phys. Rev.* **B51** (1995) 14, 103.
4. M. R. Ibarra, P. A. Algarabel, C. Marquina, J. Blasco and J. García, *Phys. Rev. Lett.* **75** (1995) 3541.
5. R. von Helmolt, J. Wecker, B. Holzapfel, L. Schultz and K. Samwer, *Phys. Rev. Lett.* **71** (1993) 2331.
6. S. Jin, T. H. Tiefel, M. McCormack, R. R. Fastnacht, R. Ramesh and L. H. Chen, *Science* **264** (1994) 413.
7. J. W. Lynn, R. W. Erwin, J. A. Borchers, Q. Huang, A. Santoro, J.-L. Peng and Z. Y. Li, *Phys. Rev. Lett.* **76** (1996) 4046.
8. H. Y. Hwang, S.-W. Cheong, P. G. Radaelli, M. Marezio and B. Batlogg, *Phys. Rev. Lett.* **75** (1995) 914.

9. W. Archibald, J.-S. Zhou and J. B. Goodenough, *Phys. Rev.* **B53** (1996) 14, 445.
10. M. C. Martin, G. Shirane, Y. Endoh, K. Hirota, Y. Moritomo and Y. Tokura, *Phys. Rev.* **B53** (1996) 14, 285.
11. S. E. Lofland, V. Ray, P. H. Kim, S. M. Bhagat, M. A. Mannheimer and S. D. Tyagi, *Phys. Rev.* **B55** (1997) 2749.
12. J. Mira, J. Rivas, F. Rivadulla, C. Vázquez Vázquez and M. A. López Quintela, *Phys. Rev.* **B60** (1999) 2998.
13. J. Mira, J. Rivas, M. Vázquez, J. M. García-Beneytez, J. Arcas and R. D. Sánchez, *Phys. Rev.* **B59** (1999) 123.
14. S. K. Banerjee, *Phys. Lett.* **12** (1964) 16.
15. L. D. Landau, *Zh. Eksperim. i Teor. Fiz.* **7** (1937) 19, 627.
16. E. M. Lifshitz, *Zh. Eksperim. i Teor. Fiz.* **11** (1941) 269.
17. V. L. Ginzburg, *Zh. Eksperim. i Teor. Fiz.* **17** (1947) 833.
18. S. V. Vonsovskii, *Izv. Akad. Nauk. SSSR* (*Ser. Fiz*) **11** (1947) 485.
19. C. P. Bean and D. S. Rodbell, *Phys. Rev.* **126** (1962) 104.
20. J. Mira, J. Rivas, F. Rivadulla and M. A. López-Quintela, *Physica* **B320** (2002) 23.
21. J. Mira and J. Rivas, *Recent Res. Devel. Magnetics* **1** (2000) 1.
22. $M^{1/\beta}$ versus $(H/M)^{\gamma}$ plots, being β and γ the critical exponents of the magnetic phase transition. In Refs. 15 and 16 the authors use or arrive to mean field critical exponents, i.e. $\beta = 0.5$, $\gamma = 1$; therefore, in practice they are M^2 versus (H/M) plots, which constitutes a Banerjee plot with swapped axes.
23. S. E. Lofland, S. M. Bhagat, K. Ghosh, R. L. Greene, S. G. Karabashev, D. A. Shulyatev, A. A. Arsenov and Y. Mudovskii, *Phys. Rev.* **B56** (1997) 13, 705.
24. Ch. V. Mohan, M. Seeger, H. Kronmüller, P. Murugaraj and J. Maier, *J. Magn. Magn. Mater.* **183** (1998) 348.
25. P. Velasco, J. Mira, F. Guinea, J. Rivas, M. J. Martínez-Lope, J. A. Alonso and J. L. Martínez, *Phys. Rev.* **B66** (2002) 104412.
26. J. Mira, J. Rivas, L. E. Hueso, F. Rivadulla, M. A. López Quintela, M. A. Señarís Rodríguez and C. A. Ramos, *Phys. Rev.* **B65** (2001) 024418.
27. C. A. Ramos, H. R. Salva, R. D. Sánchez, M. Tovar, F. Rivadulla, J. Mira, J. Rivas, M. A. López-Quintela, L. E. Hueso, M. Saint-Paul, P. Lejay and Y. Tokura, *J. Magn. Magn. Mater.* **226–230** (2001) 582.
28. J. B. Goodenough, *J. Appl. Phys.* **81** (1997) 5330.
29. J. B. Goodenough and J. M. Longo, *Landolt-Börnstein Tabellen*, Vol. III/4 (Springer, Berlin, 1970).
30. D. Louca, T. Egami, E. L. Brosha, H. Röder and A. R. Bishop, *Phys. Rev.* **B56** (1997) R8475.
31. J.-S. Zhou and J. B. Goodenough, *Phys. Rev. Lett.* **80** (1998) 2665.
32. C. Zener, *Phys. Rev.* **82** (1951) 403.
33. P. W. Anderson and H. Hasegawa, *Phys. Rev.* **100** (1955) 675.
34. P. G. de Gennes, *Phys. Rev.* **118** (1960) 141.
35. J. B. Goodenough, *Aust. J. Phys.* **52** (1999) 155.
36. M. Viret, H. Glättli, C. Fermon, A. M. de Leon-Guevara and A. Revcolevschi, *Europhys. Lett.* **42** (1998) 301.
37. J. Mira, J. Rivas, L. E. Hueso, F. Rivadulla and M. A. López-Quintela, *J. Appl. Phys.* **91** (2002) 8903.
38. Z. B. Guo, Y. W. Du, J. S. Zhu, H. Huang, W. P. Ding and D. Feng, *Phys. Rev. Lett.* **78** (1997) 1142.
39. J. Mira, A. Fondado, L. E. Hueso, J. Rivas, F. Rivadulla and M. A. López Quintela, *Phys. Rev.* **B61** (2000) 5857.

40. H. Röder, J. Zang and A. R. Bishop, *Phys. Rev. Lett.* **76** (1996) 1356.
41. G.-M. Zhao, K. Conder, H. Keller and K. A. Müller, *Nature* **381** (1996) 676.
42. P. G. Radaelli, G. Iannone, M. Marezio, H. Y. Hwang, S.-W. Cheong, J. D. Jorgensen and D. N. Argyriou, *Phys. Rev.* **B56** (1997) 8265.
43. M. M. Savosta, V. A. Borodin, P. Novák, Z. Jirák, J. Hejtmánek and M. Marysko, *Phys. Rev.* **B57** (1998) 13, 379.
44. J. B. Goodenough, *Nature* **386** (1997) 229.
45. A. Moreo, S. Yunoki and E. Dagotto, *Science* **283** (1999) 2034.
46. E. Dagotto, T. Hotta and A. Moreo, *Phys. Reports* **344** (2001) 1.
47. J. Mira, J. Rivas, A. Moreno-Gobbi, M. Pérez Macho, G. Paolini and F. Rivadulla, *Phys. Rev.* **B68** (2003) 092404.
48. S. Nowick and B. S. Berry, *Anelastic Relaxation in Crystalline Solids* (Academic Press, New York, 1972).
49. A. Moreno-Gobbi and J. A. Eiras, *J. Phys.: Condens. Matter* **12** (2000) 859.
50. M. M. Savosta, P. Novák, Z. Jirák, J. Hejtmánek and M. Marysko, *Phys. Rev. Lett.* **79** (1997) 4278.
51. A. P. Ramírez, P. Schiffer, S.-W. Cheong, C. H. Chen, W. Bao, T. T. M. Palstra, P. L. Gammel, D. J. Bishop and B. Zegarski, *Phys. Rev. Lett.* **76** (1996) 3188.
52. C. Zhu, R. Zheng, J. Su and J. He, *Appl. Phys. Lett.* **74** (1999) 3504.
53. F. Cordero, C. Castellano, R. Cantelli and M. Ferretti, *Phys. Rev.* **B65** (2002) 012403.
54. B. Juffe, in *Piezoelectric Ceramics* (Academic Press, New York, 1971).
55. D. Viehland, S. J. Jang and L. E. Cross, *J. Appl. Phys.* **68** (1990) 2916.
56. Z. G. Lu and G. Calvarin, *Phys. Rev.* **B51** (1995) 2694.
57. J. M. de Teresa, M. R. Ibarra, P. A. Algarabel, C. Ritter, C. Marquina, J. Blasco, J. García, A. del Moral and Z. Arnold, *Nature* (*London*) **386** (1997) 256.
58. A. Moreo, M. Mayr, A. Feiguin, S. Yunoki and E. Dagotto, *Phys. Rev. Lett.* **84** (2000) 5568.
59. T. Kimura, Y. Tomioka, R. Kumai, Y. Okimoto and Y. Tokura, *Phys. Rev. Lett.* **83** (1999) 3940.
60. V. Podzorov, C. H. Chen. M. E. Gershenson and S.-W. Cheong, *Europhys. Lett.* **55** (2001) 411.
61. N. D. Mathur, *Nature* **400** (1999) 405.
62. F. Rivadulla, M. A. López-Quintela, J. Mira and J. Rivas, *Phys. Rev.* **B64** (2001) 052403.
63. M. A. Señarís Rodríguez and J. B. Goodenough, *J. Solid State Chem.* **118** (1995) 323.
64. J. Mira, J. Rivas, R. D. Sánchez, M. A. Señarís Rodríguez, D. Fiorani, D. Rinaldi and R. Caciuffo, *J. Appl. Phys.* **81** (1997) 5753.
65. R. Caciuffo, J. Mira, J. Rivas, M. A. Señarís Rodríguez, P. G. Radaelli, F. Carsughi, D. Fiorani and J. B. Goodenough, *Europhys. Lett.* **45** (1999) 399.
66. R. Caciuffo, D. Rinaldi, G. Barucca, J. Mira, J. Rivas, M. A. Señarís Rodríguez, P. G. Radaelli, D. Fiorani and J. B. Goodenough, *Phys. Rev.* **B59** (1999) 1068.
67. G. Baio, G. Barucca, R. Caciuffo, D. Rinaldi, J. Mira, J. Rivas, M. A. Señarís Rodríguez and D. Fiorani, *J. Phys.: Condens. Matter* **12** (2000) 9761.
68. J. Mira, J. Rivas, G. Baio, G. Barucca, R. Caciuffo, D. Rinaldi, D. Fiorani and M. A. Señarís Rodríguez, *J. Appl. Phys.* **89** (2001) 5606.
69. F. Heusler, *Z. Angew. Chem.* **17** (1904) 260.
70. S. Hilpert and T. Dieckmann, *Ber. Deut. Chem. Ges.* **44** (1911) 2378.
71. L. F. Bates, *Proc. Roy. Soc.* (*London*) **A117** (1928) 680.
72. A. Serres, *J. Phys. Radium* **8** (1947) 146.

73. C. Guillaud, *J. Phys. Radium* **12** (1951) 223.
74. B. T. M. Willis and H. P. Rooksby, *Proc. Phys. Soc.* (*London*) **B67** (1954) 290.
75. M. Menyuk, J. A. Kafalas, K. Dwight and J. B. Goodenough, *Phys. Rev.* **177** (1969) 942.
76. L. F. Bates, *Philos. Mag.* **8** (1929) 714.
77. R. H. Wilson and J. S. Kasper, *Acta Cryst.* **17** (1964) 95.
78. J. B. Goodenough, Influence of metal-metal bonding on structures derived from NiAs structure, MIT technical report, No. 345 (1964).
79. J. B. Goodenough and J. A. Kafalas, *Phys. Rev.* **157** (1967) 389.
80. V. A. Chernenko *et al.*, *J. Appl. Phys.* **85** (1999) 7833.
81. J. Mira, F. Rivadulla, J. Rivas, A. Fondado, T. Guidi, R. Caciuffo, E. Carsughi, E. G. Radaelli and J. B. Goodenough, *Phys. Rev. Lett.* **90** (2003) 097203.
82. S. Shimomura *et al.*, *J. Phys. Soc. Jpn.* **68** (1999) 1943.
83. J. S. Zhou, H. Q. Yin and J. B. Goodenough, *Phys. Rev.* **B63** (2001) 184423.
84. A. Asamitsu *et al.*, *Nature* **373** (1995) 407.
85. G. L. Liu, J. S. Zhou and J. B.Goodenough, *Phys. Rev.* **B64** (2001) 144414.